Shielding Damage Characterization in Twisted Pair Cables Using OMTDR-based Reflectometry and Inverse Problems

Wafa Ben Hassen, Moussa Kafal

Shielding Damage Characterization in Twisted Pair Cables Using OMTDR-based Reflectometry and Inverse Problems

W. Ben Hassen and M. Kafal
CEA, LIST, Laboratoire de Fiabilite et Integration Capteurs, 91191, France

Abstract— Aeronautical wiring and interconnect systems are highly exposed to severe conditions leading to serious security problems. In such systems, the predictive diagnosis of incipient faults becomes an economic and human requirement in the perspective of predictive maintenance. This paper proposes to study and develop methods and models to detect incipient faults and characterize them in wiring and interconnect systems. A model-based inversion process combined with optimization-based algorithms have formed a suitable, reliable and efficient technique for incipient fault characterization when processed with reflectometry. To do so, a shielded twisted pair cable with a shielding damage has been modeled using Finite element method and simulated using reflectometry. It consists in injecting a wideband test signal down to the cable and recording the reflected echoes at each impedance discontinuity. The analysis of the reflectometry-based measurements permits to detect and locate incipient fault. A Genetic Algorithm (GA) is then performed to estimate the fault's features such as length, width or per-unit-length parameters (RLCG), etc., which becomes equally interesting for predictive maintenance. The proposed methodology is validated by experimental results using an electronic card including Xilinx Zunq 7010 FPGA to inject/receive Orthogonal Multi-Tone Time Domain Reflectometry (OMTDR).

1. INTRODUCTION

The Electrical Wiring Interconnect System (EWIS) is a critical component in aging aircrafts due to the appearance of wiring faults that are mainly classified into hard faults (i.e., open and short circuit), incipient faults (i.e., shielding damage, pinching, etc.) and intermittent faults (i.e., arcing) [1]. Online wiring fault diagnosis is a very important domain of study since it enables monitoring the state of an operating EWIS. Within this context, Multi-Carrier Reflectometry (MCR) and its variant Orthogonal Multi-Tone Time Domain Reflectometry (OMTDR) have formed suitable candidates since the frequency band can be segregated into several frequency sub-bands using orthogonal sub-carriers in order to control the signal bandwidth and avoid forbidden bands [2, 3]. In fact, conventional reflectometry-based signals may disturb native signals active in the live network and lead to false alarms due to the cross-talk phenomena and loads' variations in electronics. Significantly, OMTDR-based diagnosis permits to detect and locate the appearance of incipient faults as soon as possible thanks to adequate real-time processing [4].

Although the analysis of the OMTDR reflectograms based on the amplitude of the fault peak reflects the severity of the fault, it does not return an estimation of the fault's degradation with time. Accordingly, a characterization of the fault's features is necessary. This includes estimating the fault's parameters such as length, resistance (R), inductance (L), capacitance (C), conductance (G), etc., which becomes equally interesting for fault prognosis solutions. This permits estimating the fault's severity thus allowing to predict its evolution with time and therefore planning a predictive maintenance. The literature related to precursor fault characterization is poor since available research work accomplished by NASA and other teams depend on complex and non-generic physics-based models [5, 6].

This paper aims at detecting, locating and characterizing incipient faults in shielded twisted pair cables using OMTDR and optimization-based algorithms. To do so, a three-dimensional numerical modeling of shielded-twisted pairs is developed and validated by a RLCG model for a stranded twisted pair including the pitch of twist and frequency dependent effects (i.e., proximity and skin effects). After that, a three-dimensional shielding damage fault is developed and integrated in the cable model. A Reflectometry-based approach is performed to obtain the fault's signature. This is followed by applying an optimization algorithm that is capable of characterizing the shielding damage fault thus estimating its length and RLCG parameters variations. The evolution of the RLCG parameter variations according to the length and width of the shielding damage are investigated in this paper. The proposed methodology is validated by experimental results using an electronic card including Xilinx Zynq 7010 FPGA to inject/receive OMTDR signals with the shielded twisted pair cables.

The remaining of the paper is organized as follows. A twisted pair cable will be modeled based on distributed per-unit length parameters and validated based on Finite Element Method (FEM) in Section 2. In Section 3, a shielding damage with different severity will be modeled and simulated for reflectometry-based signature detection. This latter will be characterized to estimate the electrical and dimensional parameters of the incipient fault. Finally, experimental results will be performed for feasibility proof where the OMTDR method will be used to detect shielding damage on a twisted pair cable and the GA will be used to characterize it.

2. TWISTED PAIR CABLE MODELING AND NUMERICAL SIMULATIONS

A twisted pair cable is a transmission line composed of two conductors spirally wound around each other to limit sensitivity to interference and cross-talk. It is widely used in the aeronautical field for Controller application not limited to the Controller Area Network (CAN) bus, MIL-STD-1553B, etc. The characteristic impedance, Z_c, of a transmission line is a function of the distributed parameters (per unit length) series Resistance R, series inductance L, shunt capacitance C, and shunt conductance G. Since reflectometry operates at high frequencies to ensure incipient fault detection, the developed model must reflect the behavior of the transmission line at high frequencies where two factors that determine the current distribution on the conductor cross-section appear. The first phenomenon is called *skin effect* and causes a concentration of the current near the outer surfaces of the cylindrical conductor [7]. The second phenomenon is called *proximity effect* and causes a resistance value greater than that of a simple skin effect [8]. In fact, when a current flows through two or more adjacent conductors, the current distribution in a conductor is affected by the magnetic flux produced by the adjacent conductors, as well as by the magnetic flux produced by the current in the conductor itself. In this paper, we note the proximity factor P that is determined according to the ratio between D and d as described in [9]. Here, D is the distance between the centers of conductors and d is the conductor's diameter.

For a twisted pair with n strands per conductor, the resistance per unit-length in (1) is calculated as follows:

$$R(f) = P\left(\frac{2n}{\pi d\delta\sigma}\right)\left(\frac{d_s}{d}\right)^2, \tag{1}$$

where d_s is the strand diameter and f is the frequency. The skin effect δ is expressed in (2) as follows:

$$\delta = \frac{1}{\sqrt{\pi\mu\sigma f}}, \tag{2}$$

where $\mu = \mu_0\mu_r$ being the dielectric permeability, σ the conductor conductivity.

The inductance per unit-length of the cable is given in (3) as follows:

$$L = \frac{\mu_0\mu_r}{\pi}\log_{10}\left(\frac{D}{d} + \sqrt{\left(\frac{D}{d}\right)^2 - 1}\right), \tag{3}$$

where μ_0 is the permeability of free space and μ_r is the relative permeability of the dielectric.

The capacity per unit-length can be described in (4) as follows:

$$C = \frac{\pi\varepsilon_0\varepsilon_{eq}}{\log_{10}\left(\frac{D}{d} + \sqrt{\left(\frac{D}{d}\right)^2 - 1}\right)}, \tag{4}$$

where, the parameter ε_0 is the permittivity of air.

The equivalent dielectric constant integrating the influence of the twist angle ε_{eq} can be calculated in Equation (5) as follows [10]:

$$\varepsilon_{eq} = 1 + q\left(\varepsilon_r - 1\right), \tag{5}$$

where ε_r is the relative permittivity and q is the twisted correction factor and is then used to adjust the dielectric constant in Equation (6) as follows [12]:

$$q = 0.45 + 10^{-3}\left(\theta \cdot \frac{180}{\pi}\right)^2. \tag{6}$$

The helical pitch angle of twist influences the dielectric constant denoted θ and is calculated in Equation (7) as follows [11]:

$$\theta = \tan^{-1}(2T\pi D), \tag{7}$$

where T is the number of twists per meter.

The conductance per unit length G is given in (8) as:

$$G(f) = 2\pi f C \tan\delta, \tag{8}$$

where $\tan\delta$ is the tangent of the dielectric loss and depends on the frequency.

The characteristic impedance $Z_c(f)$ is defined as follows:

$$Z_c(f) = \sqrt{\frac{R + j2\pi fL}{G + j2\pi fC}}. \tag{9}$$

The propagation constant $\gamma(f)$ is given by:

$$\gamma(f) = \sqrt{(R + j2\pi fL)\,(G + j2\pi fC)}. \tag{10}$$

In order to validate the distributed parameters model, a 3D electromagnetic model of the STP is developed using the FEM method as shown in Figure 1. The model consists of 19 copper strands per conductor. The diameter of one strand is 0.15 mm. The diameter of the conductor is $d = 0.75$ mm. The conductor is covered by a thin layer of Teflon insulation whose thickness is 0.08 mm. The insulation is Teflon (PTFE) with a permittivity $\varepsilon_r = 2.1$, a permeability $\mu_r = 1$ and the angle of loss $\delta = 0.0002$. The distance between the two conductors is $D = 0.95$ mm and the number of twist steps is 100 per meter. Both wires are covered by an annealed copper shielding. The thickness of the shielding is 0.07 mm. Finally, there is an outer Teflon sheath which envelops all the components of thickness 0.08 mm. The length of the model is 1 m. A local mesh is performed, as shown in Figure 1, with a step width in absolute value as follows: $x = 0.1$ mm, $y = 0.04$ mm and $z = 0.04$ mm. The total number of meshes is 37 004 352. The 19 strands per conductor are connected to a central point through 19 lines with perfect conductivity and lengths of 0.5 mm. A port with a 50 Ω impedance connects the two conductors through the center points to inject/receive test signals.

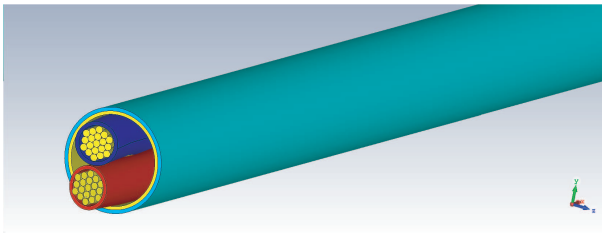

Figure 1: Shielding twisted pair modeling.

The RLCG-based model is developed and its results are compared to those of the FEM-based model. To do so, the proximity factor $P = 2.1$ is determined directly from the curve provided in [9] for a ratio $(\frac{D}{d}) = 1.2$. To reconstruct the reflectogram from the secondary parameters calculated on the basis of R, L, C and G, the transfer function expressed as follows can be used:

$$H(f) = \Gamma_E + \frac{(1 - \Gamma_E^2)\Gamma_L e^{-2\gamma(f)l}}{1 + \Gamma_E \Gamma_L e^{-2\gamma(f)l}}, \tag{11}$$

where l is the length of the cable, Γ_E and Γ_L are, respectively, the reflection coefficients at the input and output of the line.

The reflection coefficient Γ_E at the input of the line is calculated as follows:

$$\Gamma_E = \frac{Z_c - Z_0}{Z_0 + Z_c}, \tag{12}$$

with Z_0 is the impedance of the generator. In this case, it is considered equal to 50 Ω. In the case of an open circuit at the end of the line, the reflection coefficient is $\Gamma_L = 1$.

Figure 2 shows the TDR reflectograms of the RLCG-based model and the 3D EM model. For these simulations, the used bandwidth ranged from DC to 1 GHz and the width of the Gaussian pulse, used as test signal, is 1 ns. The coefficient of correlation between the two reflecotgrams from the RLCG-based model and 3D-based model is equal to 0.9881. One can thus consider that the coefficient of correlation is high and can validate the model with distributed constants developed previously in the case of a twisted pair. The computed R, L, C and G parameters of the healthy cable permit the incipient fault characterization later on.

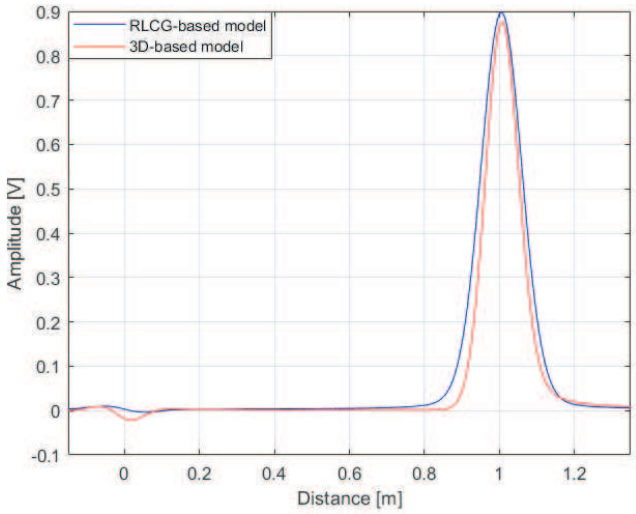

Figure 2: Time domain reflectograms of the RLCG model and 3D model of the twisted pair.

3. SHIELDING DAMAGE MODELING AND CHARACTERIZATION

An incipient fault characterization algorithm is developed in this paper as shown in the flow chart of Figure 3. After detecting and locating the incipient fault on the resulting reflectogram, it is proposed to determine its per-unit length features such as the resistance, the capacitance, the inductance, the length and the position. For this, the developed algorithm proposes to solve an

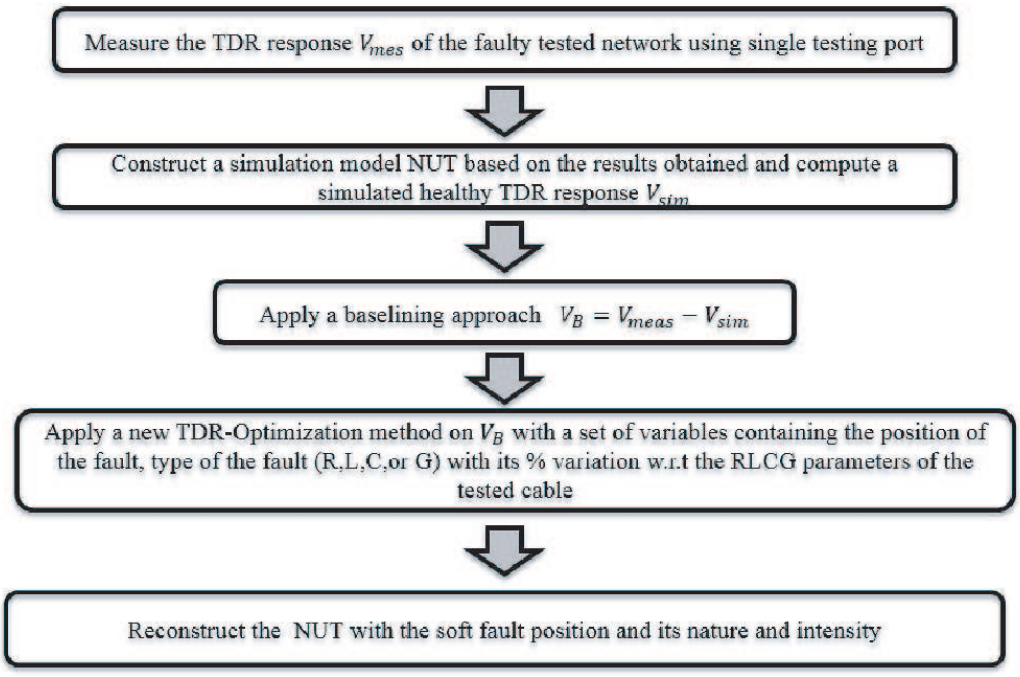

Figure 3: Flow chart of the algorithm for the characterization of the incipient fault.

inverse problem where the optimization techniques constitute an excellent candidate (i.e., particle swarm, etc.).

In this paper, the GA algorithm is considered thanks to its efficiency in terms of computation time and simplicity. It has been applied with success to the blind reconstruction of black-boxed unknown complex wire networks [13].

The proposed algorithm considers three set of variables to run. The first set corresponds to the nature of the fault where a vector $N = \{R, L, C, G\}$ including the starting values (in the case of a healthy cable): the resistance R, the inductance L, the capacitance C and the conductance G. The second is the fault parameters $D = \{L_f, p_f\}$, where L_f is the fault length and p_f is the fault position. The last set of variables is the variation denoted Δ_v with respect to the RLCG parameters of the cable under test. Here, Δ_v is a vector of 4 elements including the variation of R, the variation of L, the variation of C and the variation of G. At the output, one can define, for example, the resistance of the defect $R_d = R(1 + \Delta_v(1)/100)$.

In order to measure the TDR response V_{mes} of the faulty test network using a single testing port, it is proposed to model a shielding damage on the twisted pair developed in Figure 2 and then, simulated using time domain reflectometry.

In this section, it is proposed to study the effect of increasing the width l and the length L of the shielding damage noted T_2 in terms of RLCG parameters. The Figures 4, 5 and 6 show, respectively, the incipient fault T_2 with width $l = 1.78\,\text{mm}$, $l = 2\,\text{mm}$ and $l = 2.22\,\text{mm}$. In all three cases, the length of the fault remains fixed where $L = 5\,\text{mm}$. Figure 11 shows the electrical signatures of the shielding damage T_2 with different severity as presented in Figures 4, 5 and 6.

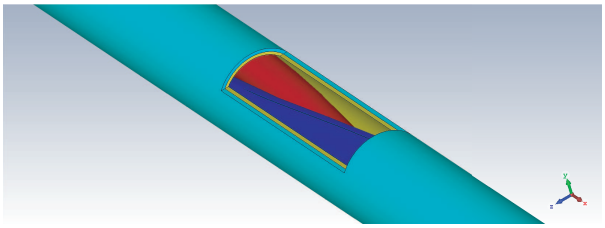

Figure 4: Model of fault T_2 with $l = 1.78\,\text{mm}$.

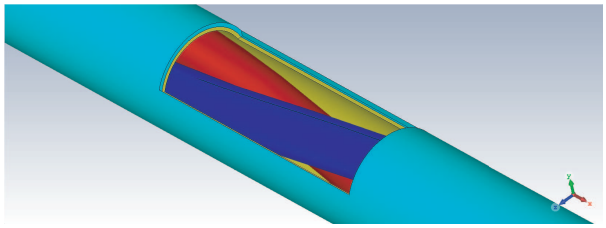

Figure 5: Model of fault T_2 with $l = 2\,\text{mm}$.

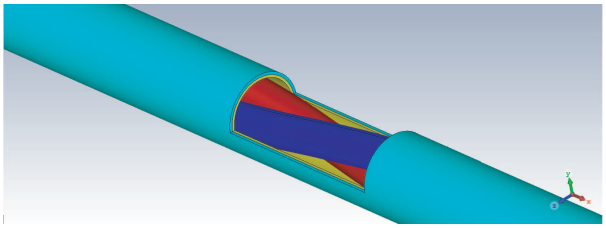

Figure 6: Model of fault T_2 with $l = 2.22\,\text{mm}$.

For these simulations, the maximum frequency of the signal is 1 GHz and time domain reflectometry is used with a Gaussian pulse considered as a test signal. In the proposed algorithm, the signature for each case as shown in Figure 11 is denoted as V_{mes}. The TDR response noted V_{sim} is obtained based on the parameters R, L, C and G computed in Section 2. After that, a baselining is performed to extract the incipient fault signature noted V_B where $V_B = V_{mes} - V_{sim}$. Then, a set of variables containing the position of the fault, the type of the fault with its variation according to R, L, C and G parameters obtained in the healthy case and V_{sim} is simulated according to Equation (11). The GA algorithm is performed on V_B until reaching the defined threshold.

In the case of a shielding damage with width 1.78 mm, the variation of the resistance R is 63%, the inductance L is 40% and the capacitance C is 5%. The fault length is $l_f = 4\,\text{mm}$ and the fault position p_f is 510 mm. The computational time using a state-of-art computer is 111.776031 seconds. Based on the R_d, L_d and C_d parameters obtained from the GA algorithm, the impedance of the calculated fault is $Z_d = 82.62\,\Omega$ and the impedance of the cable $Z_c = 71.42\,\Omega$. The fault T_2 with width 1.78 mm thus introduces an impedance variation $11.2\,\Omega$ and hence, a reflection coefficient $\Gamma = (Z_d - Z_c)/(Z_d + Z_c) = 0.072$.

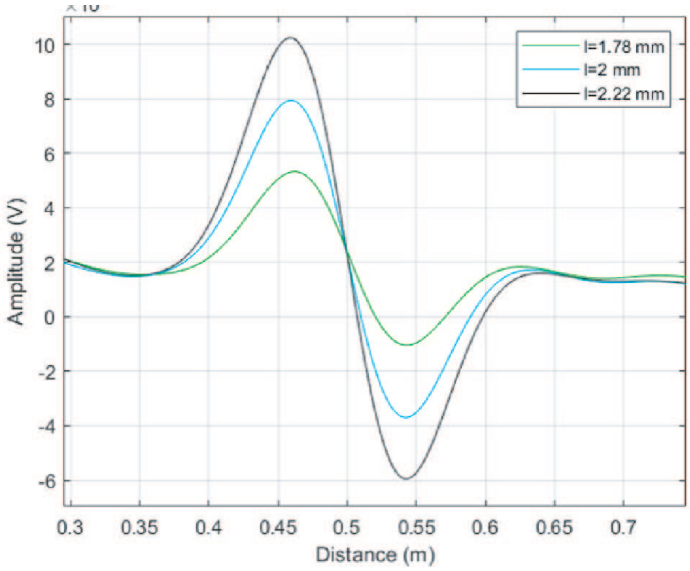

Figure 7: Signatures of fault T_2 at different widths.

In the case of shielding damage with width 2 mm, the variation of the resistance R is 81%, the inductance L is 65% and the capacitance C is 8%. The fault length is $l_f = 5\,\text{mm}$ and the fault position p_f is 500 mm. The computational time is 120.822088 s. Based on the parameters R_d, L_d and C_d obtained from the GA, the impedance of the calculated fault is $Z_d = 88.42\,\Omega$. The fault T_2 with width 2 mm thus introduces an impedance variation $17\,\Omega$ and thereafter, a reflection coefficient $\Gamma = (Z_d - Z_c)/(Z_d + Z_c) = 0.106$.

In the case of shielding damage with width 2.22 mm, the variation of the resistance R is 91%, the inductance L is 82% and the capacitance C is 7%. The fault length is $l_f = 5\,\text{mm}$ and the fault position p_f is 510 mm. The computational time is 100.6215 s. Based on the R_d, L_d and C_d parameters obtained from the GA, the impedance of the calculated fault is $Z_d = 93.31\,\Omega$ leading to impedance variation $21.89\,\Omega$ and thereafter, a reflection coefficient $\Gamma = (Z_d - Z_c)/(Z_d + Z_c) = 0.132$.

The Figures 8, 9 and 10 show the signatures of the fault T_2 with width 1.78 mm, 2 mm and 2.22 mm, respectively, reconstructed from the RLCG parameters calculated by the genetic algorithm. The correlation coefficient is used to estimate the resemblance between the reconstructed signature from the results of the genetic algorithm and that resulting from the developed models.

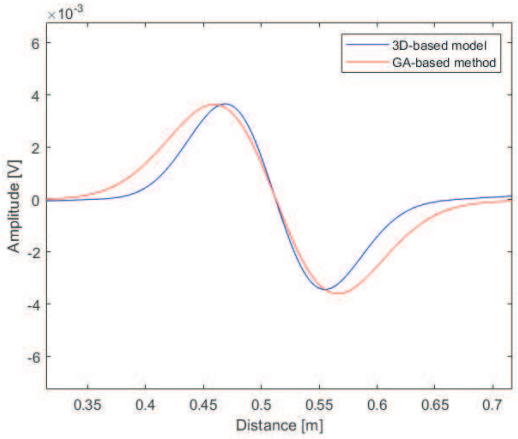

Figure 8: Signatures of the reconstructed and simulated fault with width 1.78 mm.

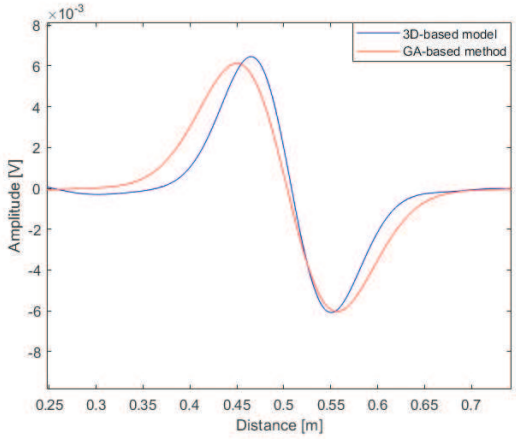

Figure 9: Signatures of the reconstructed and simulated fault with width 2 mm.

The Table 1 permits to summarize the R, L and C parameters variation in terms of fault length L with length $L = 5\,\text{mm}$. The parameter G is considered constant in this study. It is possible to

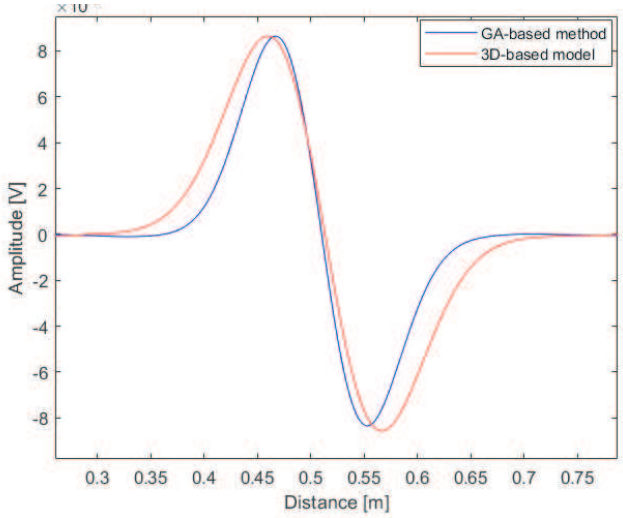

Figure 10: Signatures of the reconstructed and simulated fault with width 2.22 mm.

notice that the increase of the width of the shielding damage causes an increase in variation of a characteristic impedance of a cable in the defective zone passing from 11.2 Ω with $l = 1.78$ mm, 17 Ω with $l = 2$ mm and 21.89 Ω with $l = 2.22$ mm.

Table 1: The estimated parameters of the shielding damage for different widths.

Width of the fault	ΔR	ΔL	ΔC	p_f	l_f	ΔZ_c
$l = 1.78$ mm	63%	40%	5%	510 mm	4 mm	11.2 Ω
$l = 2$ mm	81%	65%	8%	500 mm	5 mm	17 Ω
$l = 2.22$ mm	91%	82%	7%	510 mm	5 mm	21.89 Ω

The characterization of the shielding damage also shows an increase in the resistance R and the inductance L which comes with the increase in the width. The characterization of the incipient fault shows that the capacitance does not vary significantly when the fault width increases.

It is now proposed to study the effect of increasing the length of the shielding damage on the variation of its parameters. The Table 2 permits to summarize the R, L and C parameters variation in terms of the fault length L with width $l = 2$ mm. It may be noted that the increase in the length of the fault does not modify the variation of the per-unit length parameters of the cable, and subsequently the variation of its secondary parameters since the impedance of the fault T_2 of length 10 mm and 15 mm is, respectively, $Z_d = 78.74\,\Omega$ and $Z_d = 78.23\,\Omega$. However, the increase of the fault length l increases the amplitude of the fault signature based on reflectometry as shown in Equation (11).

Table 2: The estimated parameters of the shielding damage for different lengths.

Length of the fault	ΔR	ΔL	ΔC	p_f	l_f	ΔZ_c
$L = 10$ mm	12%	24%	2%	510 mm	9 mm	7.32 Ω
$L = 15$ mm	8%	20%	2%	510 mm	14 mm	6.81 Ω

4. EXPERIMENTAL RESULTS

This section aims at proving the feasibility of the proposed methodology on OMTDR-based measurements. The experimental setup consists of an electronic board for OMTDR-based measurement and a shielded twisted pair TWINLINK 50 FA with length 30 m. A −5 mm long, 3 mm wide-shielding damage is present at 10 m from the injection point as shown in Figure 11. The length of the cable under test (CUT) is 30 m.

Figure 11: Shielding damage with width 5 mm at 10 m from the electronic board.

An OMTDR signal consisting of 128 sub-carriers is considered on a total bandwidth ranging from 300 kHz to 1.5 GHz with 2048 samples (number of phases is 16). Both analog-to-digital and digital-to-analog converters sample on a 10-bit dynamic and sample at a frequency of 188 MHz. A simplified model of an OMTDR system performing wire diagnosis is presented in Figure 12 [14].

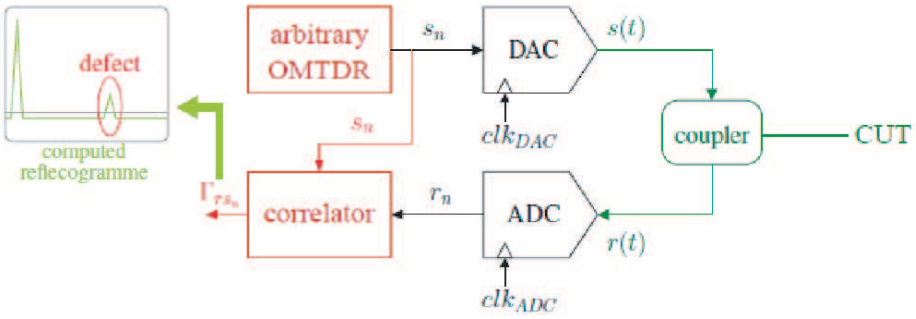

Figure 12: Schematic diagram of a standard OMTDR reflectometry based wire diagnosis system performing correlation between the injected signal $s(t)$ and the received signal $r(t)$ to detect faults.

The proposed method has been applied on the OMTDR-based reflectogram to evaluate the

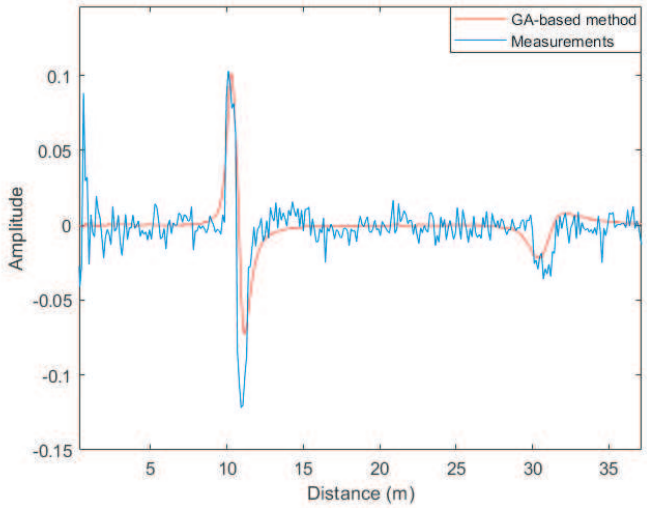

Figure 13: Differential reflectogram reconstructed based on GA method and measurements.

per-unit length parameters of the shielding damage in Figure 11. The variation of the resistance R is 90%, the inductance L is 170% and the capacitance C is 5% in this case. Figure 13 shows the reconstructed reflectogram based on GA algorithm (red curve) and the differential measured reflectogram (blue curve) where a difference is applied between the measured reflectogram and the reference, the state of healthy cable. It is obvious that the measurements present a positive peak at the beginning of the reflectogram which is not the case for the reconstructed reflectogram. This difference may be explained by the use of the reference since this latter may change in practice due to the cable moving for example.

5. CONCLUSION

In this paper, the per-unit-length parameters of shielding damage with different severities in terms of length and width has been modeled and characterized using genetic algorithm integrated with time domain reflectometry for feasibility proof. Numerical simulations results validate the parameters derived from the genetic algorithm. After that, the proposed methodology has been applied on OMTDR-based measurement that have been performed using an electronic board and a twisted pair cable with a shielding damage. Experimental results show that the proposed methodology permit to characterize the incipient faults. This latter permits to ensure predictive maintenance.

REFERENCES

1. Auzanneau, F., "Wire troubleshooting and diagnosis: Review and perspectives," *Progress In Electromagnetics Research B*, Vol. 49, 253–280, 2013.
2. Amini, P., C. Furse, and B. Farhang-Boroujeny, "Filterbank multicarrier reflectometry for cognitive live wire testing," *IEEE Sensors Journal*, Vol. 9, No. 12, 1831–1837, 2009.
3. Incarbone, L., S. Evain, W. Ben Hassen, F. Auzanneau, et al., "OMTDR based integrated cable health monitoring system SmartCo: An embedded reflectometry system to ensure harness auto-test," *IEEE Conference on Industrial Electronics and Applications (ICIEA)*, 1761–1765, June 2015.
4. Ben Hassen, W., M. G. Roman, B. Charnier, et al., "Embedded omtdr sensor for small soft fault location on aging aircraft wiring systems," *Procedia Engineering*, Vol. 168, 1698–1701, 2016.
5. Schuet, S., A. T. Dogan, and W. R. Kevin, "Physics-based precursor wiring diagnostics for shielded-twisted-pair cable," *IEEE Trans. Instrumentation and Measurement*, Vol. 64, No. 2, 378–391, 2015.
6. Manet, A., F. Loete, and F. Genoulaz, "Equivalent circuit model of soft shield defects in coaxial cables using numerical modelling," *IEEE Transactions on Electromagnetic Compatibility*, Vol. 59, No. 2, 533–536, April 2017.
7. Wheeler, H. A., "Formulas for the skin effect," *Proceedings of the IRE*, Vol. 30, No. 9, 412–424, 1942.
8. Ferkal, K., M. Poloujadoff, and E. Dorison, "Proximity effect and eddy current losses in insulated cables," *IEEE Transactions on Power Delivery*, Vol. 11, No. 3, 1171–1178, 1996.
9. Smith, G., "The proximity effect in systems of parallel conductors and electrically small multiturn loop antennas," No. TR-624, Div. of Engineering and Applied Physics, Harvard Univ. Cambridge, MA, 1971.
10. Kasthala, S. and G. P. Venkatesan, "Experimental verification of distributed parameters on indian residential networks for power line communication," *International Journal of Engineering & Technology*, Vol. 8, No. 6, 2012.
11. Lefferson, P., "Twisted magnet wire transmission line," *IEEE Transactions on Parts, Hybrids, and Packaging*, Vol. 7, No. 4, 148–154, 1971.
12. Truong, T. K., "Twisted-pair transmission-line distributed parameters," *EDN Mag.*, 2000.
13. Kafal, M., J. Benoit, and C. Layer, "A joint reflectometry-optimization algorithm for mapping the topology of an unknown wire network," *IEEE SENSORS*, 1–3, 2017.
14. Cabanillas, E., M. Kafal, and W. Ben-Hassen, "On the implementation of embedded communication over reflectometry-oriented hardware for distributed diagnosis in complex wiring networks," *IEEE AUTOTESTCON*, 1–6, September 2018.